

## Heat treatment and CVD aluminizing of Ni-base René 80 superalloy

**M. Pytel\*, M. Góral, A. Nowotnik, J. Sieniawski, M. Drajewicz, W. Ziaja**

Department of Materials Science, The Faculty of Mechanical Engineering and Aeronautics, Rzeszow University of Technology, Al. Powstańców Warszawy 12, 35-959 Rzeszów, Poland

\* Corresponding e-mail address: mpytel@prz.edu.pl

Received 09.01.2012; published in revised form 01.03.2012

### Manufacturing and processing

#### ABSTRACT

**Purpose:** This work presents the results of microstructure investigations which were carried out on Ni-base René 80 polycrystalline superalloy.

**Design/methodology/approach:** Polycrystalline cast rods have been used in the studies. The heat treatment processes were conducted in ALD High Temperature Vacuum Furnace at 1204°C for 2 h, in Ar atmosphere followed by cooling to room temperature. The aluminizing processes were conducted by use of CVD method on as cast samples and after homogenizing-solution annealing. The diffusion low activity aluminide coatings have been produced using the CVD IonBond BPXPR0325S apparatus at various temperatures, for 4 h and applying different values of: flow rate of HCl through the outer AlCl<sub>3</sub> generator and pressure in main retort in H<sub>2</sub> atmosphere. The microstructure investigations were conducted using scanning electron microscope. To the purpose of analysis of the chemical composition an X-ray microanalysis technique was applied with the dispersion of the energy (EDS) using of Thermo and Noran equipment.

**Findings:** It was found that samples without heat treatment had the typical cast microstructure with many areas of the  $\gamma$ - $\gamma'$  eutectic, after heat treatment process the microstructure was homogenized, i.e. the eutectic  $\gamma$ - $\gamma'$  has been dissolved, MC-type carbides were precipitated on the grain boundaries and the chemical composition was balanced. It was found also that after homogenizing heat treatment the samples had the thicker coating and had more homogenous additive and diffusion layer than the samples with as-cast microstructure.

**Research limitations/implications:** Results will be used for further steps which will consist of CVD process and other different heat treatment.

**Practical implications:** This CVD method will be used in the future for the production of modified aluminide bond coats on single crystal Ni-base superalloys underlying the ceramic EB-PVD or LPPS top coatings.

**Originality/value:** In the future the production of chemical vapor deposited platinum (or Pd, Zr, Hf) aluminide diffusion coatings on nickel base superalloy substrate are planned.

**Keywords:** Superalloys; Heat treatment; CVD aluminizing; Protective coatings; Diffusion coatings

#### Reference to this paper should be given in the following way:

M. Pytel, M. Góral, A. Nowotnik, J. Sieniawski, M. Drajewicz, W. Ziaja, Heat treatment and CVD aluminizing of Ni-base René 80 superalloy, Journal of Achievements in Materials and Manufacturing Engineering 51/1 (2012) 30-38.

## 1. Introduction

René 80 (General Electric Company trademark) is nickel based superalloy manufactured as a polycrystalline, equiaxed or directionally solidified alloy by use of investment casting method. It is used in aerospace industry for production of such elements of jet engines as blades and vanes of the first and second stage of the turbine. This superalloy is characterized by very good properties, such as heat resistance, high temperature creep resistance, good tensile properties and thermal fatigue strength [1-4].

René 80 is a precipitation hardened alloy with complex chemical composition (Table 1). Its microstructure after casting process consists of many dendrites of  $\gamma$  phase characterized by microsegregation and inhomogeneity with primary  $\gamma'$  precipitates within. In the interdendritic regions  $\gamma$ - $\gamma'$  eutectic, precipitates of  $\gamma'$  phase and MC type carbides are present. In order to homogenize chemical composition of the alloy and to eliminate as-cast microstructure (dendritic microsegregation,  $\gamma$ - $\gamma'$  eutectic) it is necessary to apply homogenizing-solution heat treatment. Tensile strength in the precipitate hardened alloys depends on volume fraction of  $\gamma'$  phase ( $V_V - \gamma'$ ). In superalloys with high volume fraction of  $\gamma'$  phase the optimum mechanical properties are usually achieved as a result of the two-step aging. The high temperature aging precedes the medium temperature aging. Application of such heat treatment processes enables control of the microstructure. In order to obtain good high temperature creep resistance moderately fine precipitates of primary  $\gamma'$  phase ( $\sim 0.25 - 0.5 \mu\text{m}$ ) are preferred over the ultrafine or coarse ones, as well as fine secondary precipitated  $\gamma'$  phase and coarse-grained  $\gamma$  phase microstructure. In casting alloys morphology of the  $\gamma'$  precipitates may vary due to the effect of segregation and cooling rate variation, especially smaller particles of  $\gamma'$  phase are formed in the dendrite cores while coarser  $\gamma'$  particles and  $\gamma$ - $\gamma'$  eutectic, quite often in the form of colonies, within the interdendritic regions. The main purpose of the two stage aging in nickel based superalloys besides to the control of the size of  $\gamma'$  or  $\gamma''$  precipitates is also control of the morphology of carbides formed as the precipitates at grain boundaries. It is worth mentioning that in columnar grain directionally solidified (CG-DS) alloys for example MAR M200 + Hf direct relationship between the creep-rupture strength at  $980^\circ\text{C}$  and volume fraction  $V_V$  of fine  $\gamma'$  precipitates was established [4]. However, it is very important to dissolve all the primary  $\gamma'$  particles and homogenize the as-cast alloy in order to uniform the microstructure of the alloy. To do this the homogenization-solution heat treatment should be properly carried out, i.e. not only above the  $\gamma'$  solvus temperature but close to the solidus temperature. Such process is called subsolidus solution heat treatment and should not result in melting the eutectic.

In order to increase solid solution hardening effect some refractory elements as W, Mo, Re and Ta are added to the superalloys [4]. It was found that the strongest effect has addition of Ta due to large size of its atoms, which diffuse towards the  $\gamma'$  phase resulting in its hardening. This is immensely important, especially in superalloys with large volume fraction of  $\gamma'$  phase (i.e.  $>50\%$ ), because the increase in the shear modulus of elasticity of  $\gamma'$  phase restrains phenomenon of dislocations cutting [1-4]. However, presence of the refractory elements implies insufficient heat resistance which can cause premature wear and

damage of the elements. In order to protect substrate material from hot corrosion and oxidation, application of the protecting coatings is often necessary.

Table 1.  
Nominal chemical composition of polycrystalline superalloy René 80

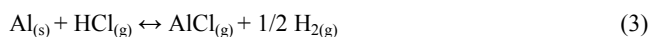
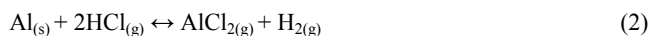
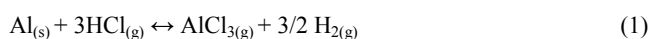
| Nominal composition, wt. % |    |     |     |      |      |      |      |      |       |       |
|----------------------------|----|-----|-----|------|------|------|------|------|-------|-------|
| Ni                         | Cr | Co  | Ti  | Al   | Mo   | W    | C    | Zr   | B     | S     |
| bal.                       | 14 | 9.0 | 5.0 | 2.98 | 3.78 | 3.78 | 0.16 | 0.02 | 0.015 | 0.001 |

Aluminide protective coatings have been used extensively in order to protect nickel based superalloys against hot corrosion and oxidation. Especially coatings based on phases from the Ni-Al binary system exhibit very good properties [5-6]. The alloys based on ordered intermetallics are very good candidate materials for elements of aircraft turbine engines.

Primary phase of that system, i.e.  $\beta$ -NiAl, possesses very high melting point  $1640^\circ\text{C}$  (at stoichiometric composition of 50% at. of aluminium), low density  $5.9 \text{ g/cm}^3$ , excellent heat resistance (even compared to other aluminides) and good mechanical properties, including high specific strength. Very good heat resistance results from the propensity to formation of protective thin layer of the aluminium oxide -  $\text{Al}_2\text{O}_3$  [5-7].

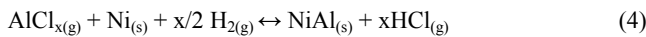
In the aerospace industry protective coatings have wide applications. These coatings have been developed because of the unsatisfactory hot corrosion resistance of the structural materials, also the nickel based superalloys [8-12]. There are many different types of protective coatings, which can be produced using various methods, for example by PVD methods such as PA-PVD (plasma assisted physical vapour deposition) or using methods producing diffusion layers, for example pack cementation method, slurry, VPA (vapour phase aluminizing) or CVD (chemical vapour deposition) [13-18].

CVD method consists in transferring aluminium from solid (e.g. mixture of aluminium granules or aluminium powders and  $\text{Al}_2\text{O}_3$  - of different proportions) to its active compounds (precursors), i.e. halides  $\text{AlCl}_3$  in a gaseous phase, which form in external generator and then transport it using gas carrier ( $\text{H}_2$ ) to the main retort (reactor chamber) to develop the coating at high temperature and at low pressure (LP CVD - low pressure chemical vapour deposition). Solid state aluminium is transformed into gaseous phase through the following chemical reactions:



where: s - solid state, g - gaseous state

In the low-activity CVD process the aluminium halides ( $\text{AlCl}_3$ ) are converted as a result of pyrolysis reaction to the subhalides, next they are deposited on the substrate and then react exothermically with substrate (Ni-based superalloy). As the consequence of the outward diffusion of Ni atoms intermetallic phase  $\beta$ -NiAl forms. The reaction of deposition can be written as:



where: s - solid phase, g - gaseous phase

Different thickness of the layers formed in the low-activity CVD process may be obtained. Many factors affect the kinetics of the coatings growth, for example temperature in the main reactor, value of the flow rate of HCl and AlCl<sub>3</sub> and also of the carrier gasses (and their suitable proportions). The diffusion aluminide coatings produced in low-activity process by use of the LP CVD method normally consist of the outer (additive) layer and diffusion zone. The outer layer ( $\beta$ -NiAl - B2 structure) may contain from 40 to around 50% at. of Al (sometimes even to 55% at. of Al). It depends on the type of the process and its parameters. As a results of the interdiffusion of the refractory elements and nickel, precipitates of various phases form in diffusion zone, including TCP phases in the secondary diffusion zone. It is necessary to recall that processes of CVD aluminizing may be also with other precursors simultaneously conducted, i.e. with ZrCl<sub>4</sub> or HfCl<sub>4</sub>. Aluminide coatings may be also modified by use of precious metals for example Pt or Pd [18-26].

## 2. Material and research methodology

### 2.1. Material

Polycrystalline superalloy René 80 was supplied in the form of cast rods 14 mm in diameter and 120 mm long. Nominal chemical composition of the alloy is presented in Table 1. Samples were cut to discs of a thickness of 4 mm. Next, they were grinded using abrasive papers ending on the grit size of 1000.

### 2.2. Heat treatment

Samples were divided into three batches. One batch of the samples was not heat treated, the second batch of samples was subjected to a homogenizing-solution heat treatment according to scheme I (Fig. 1), while additional primary aging was introduced to the heat treatment of the third batch - scheme II (Fig. 2).

The first stage of heat treatment was carried out by the following routes:

Scheme I: heating to the temperature of 1100°C at the rate of 15°C/min, then to 1205°C at the rate of 5°C/min) followed by annealing at 1205°C for 2 h and quenching in a stream of Ar to room temperature at the cooling rate of about 110°C/min.

Scheme II: The same as for I Scheme, however after homogenizing heat treatment (1205°C/2 h) cooling to the temperature of 1094°C was applied in the stream of argon within about 15 min. Next step was primary ageing treatment at 1094°C for 4 h followed by cooling to room temperature within about 10 min.

All processes of the heat treatment were being conducted using the Monotherm<sup>®</sup> Vacuum Furnace (ALD Vacuum Technologies GmbH) in high vacuum and in argon protective atmosphere at pressure  $5 \cdot 10^{-5}$  mbar ( $5 \cdot 10^{-3}$  Pa).

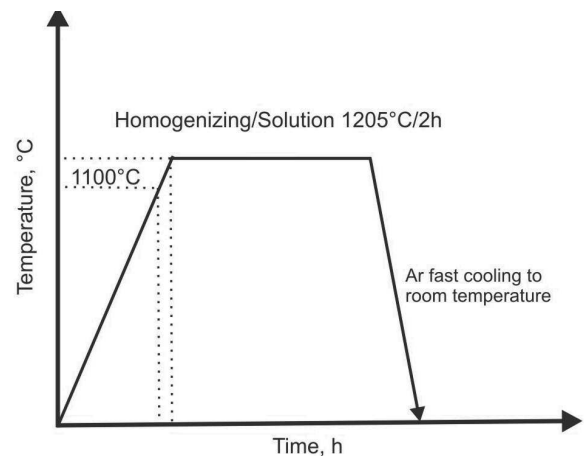


Fig. 1. Scheme of homogenizing and solution heat treatment of René 80 polycrystalline superalloy

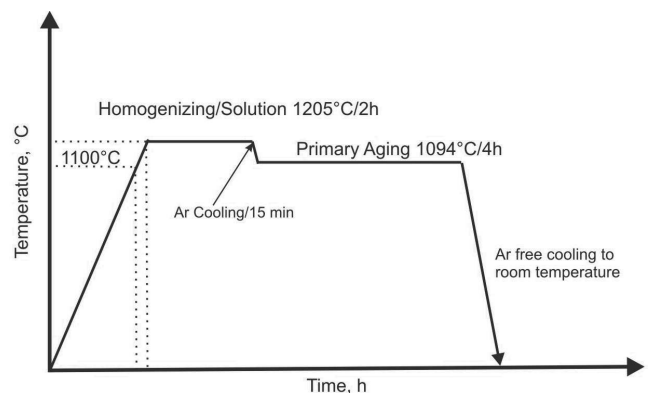


Fig. 2. Scheme of homogenizing-solution and primary aging heat treatment of René 80 polycrystalline superalloy

### 2.3. Low-activity CVD aluminizing process

For conducting the diffusion process of aluminizing BPX-Pro 325S apparatus from the Ionbond company was used. The system consists of the outside generator containing granules of aluminium by which the gaseous hydrogen chloride HCl and hydrogen H<sub>2</sub> is being let in. The hydrogen chloride plays the role of activating gas, reaction (1), so-called precursor, converting aluminium from the solid state to the gaseous state (AlCl<sub>3</sub>). Temperature at the inlet to the generator aluminium is ~350°C, in addition, the hydrogen plays the role of carrier gas. After the activation the AlCl<sub>3</sub> temperature at the outlet from the generator is about 290°C. Such the mixture of gases is supplemented with additional portion of hydrogen.

CVD processes were conducted in different conditions, i.e. varying values of the HCl flow rate, HCl/H<sub>2</sub> ratio, pressure and temperature in the main retort. All samples were aluminized by the low-activity CVD method following the routes summarized in Table 2.

Table 2.  
Heat treatment and CVD process parameters applied for René 80 superalloy

| No.  | CVD process parameters                      |  |                              |                  |      | Heat treatment |         |                             |   |
|------|---|--|------------------------------|------------------|------|----------------|---------|-----------------------------|---|
|      | Flow rate of HCL + 3nlpm* of H <sub>2</sub> | Flow rate of H <sub>2</sub> supplement | Pressure in the main reactor |                  | Time | Temperature    | As-cast | Homogenizing/ solutionizing | Homogenizing/ solutionizing + primary aging |
|      | nlpm  | nlpm                                   | mbar                         | Pa               | h    | °C             |         |                             |   |
| 1.   | 1.4   | 10                                     | 150                          | $1.5 \cdot 10^4$ | 4    | 950            | yes     | no                          | no  |
| 2.   | 1.4   | 10                                     | 150                          | $1.5 \cdot 10^4$ | 4    | 1050           | yes     | no                          | no  |
| 3.   | 0.15  | 20                                     | 150                          | $1.5 \cdot 10^4$ | 4    | 1000           | yes     | no                          | no  |
| 4.   | 0.15  | 30                                     | 150                          | $1.5 \cdot 10^4$ | 4    | 1000           | yes     | yes                         | no  |
| 5.   | 0.6   | 10                                     | 300                          | $3.0 \cdot 10^4$ | 4    | 1000           | yes     | yes                         | no  |
| 6.** | 0.5   | 10                                     | 150                          | $1.5 \cdot 10^4$ | 4    | 1050           | yes     | yes                         | yes   |

\*nlpm - Normal Liters per Minute

\*\* the samples after process were annealed in Ar at 1000°C for 2 h

## 2.4. Examinations of microstructure

Examination of the microstructure was conducted using the light microscope Nikon Epiphot 300 with the NIS-Elements V2.3 software and scanning electron microscope Hitachi S-3400N equipped with Thermo Noran EDS system for chemical composition analysis. Metallographic specimens were prepared using standard metallographic methods. Samples after the process of aluminizing were cut along the diameter and then were plated with nickel by use of electroless method. Cross sections of metallographic samples with aluminide layers were prepared by grinding with abrasive papers down to 2400 grit size followed by polishing using diamond suspensions (6, 3, 1  $\mu\text{m}$ ). For chemical composition analysis of aluminide layers unetched microsections were applied. Metallographic microsections after processes of the heat treatment were prepared applying the method which was described earlier, at the end they were polished with acidic alumina. Microsections were etched with the following reagents: Kalling's reagent (waterless number 2): 5g  $\text{CuCl}_2$  + 100 ml HCl + 100ml ethanol and the second one 10 ml  $\text{HClO}_4$  + 20 ml glycerol + 70ml ethanol

## 3. Results and discussion

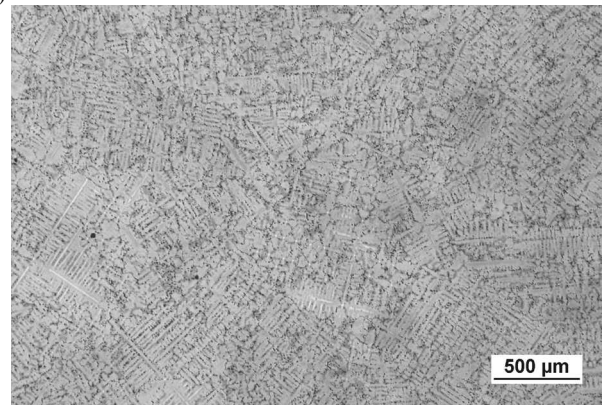
Metallographic examination of René 80 superalloy rods using the light and SEM microscopes revealed the typical casting microstructure with indications of dendritic microsegregation (Fig. 3a). The areas of  $\gamma$ - $\gamma'$  eutectic colonies were identified in the interdendritic regions (Fig. 3b).

Based on the chemical composition examinations an increased content of aluminium, titanium and nickel was found in the  $\gamma$ - $\gamma'$  eutectic (Fig. 4b). However, around eutectics segregated precipitates rich in such elements as tungsten, molybdenum, zirconium and chromium were identified. In these areas the content of nickel, titanium and aluminium was lowered.

It was found, that average size of  $\gamma'$  precipitates observed in interdendritic regions was larger than in dendrite cores. After homogenizing annealing more homogeneous microstructure was observed. Moreover the  $\gamma$ - $\gamma'$  eutectic was completely dissolved.

Large precipitates spread over grain boundaries were observed, and smaller ones were also distributed inside the grains. On the basis of an EDS analysis of the chemical composition they were identified as MC-type carbides (Fig. 6) (where M stands for W, Ti, or Mo).

a)



b)

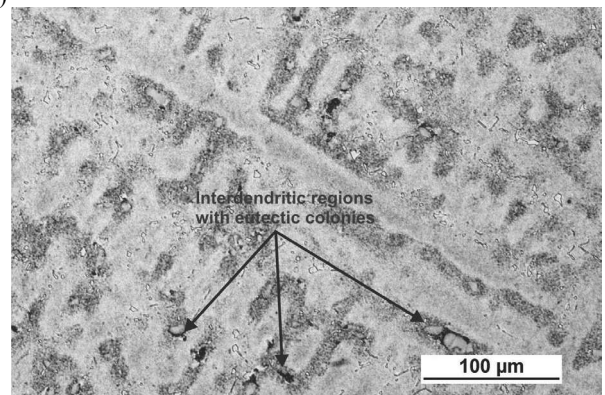


Fig. 3. Microstructure of René 80 superalloy in the as-cast state (LM - bright field) -  $\gamma$ - $\gamma'$  eutectic colonies in interdendritic regions

Table 3.

Local chemical composition of René 80 superalloy in the area of  $\gamma$  -  $\gamma'$  eutectic within interdendritic region - EDS analysis

| Area no.<br>(Fig. 4b) | Element content, wt % |       |       |      |       |      |       |       |
|-----------------------|-----------------------|-------|-------|------|-------|------|-------|-------|
|                       | Al                    | Ti    | Cr    | Co   | Ni    | Zr   | Mo    | W     |
| 1                     | 3.63                  | 11.82 | 6.08  | 6.84 | 70.47 | -    | 1.00  | 0.16  |
| 2                     | -                     | 4.79  | 28.66 | 3.98 | 23.30 | -    | 27.19 | 12.08 |
| 3                     | 3.99                  | 12.66 | 4.18  | 7.17 | 72.00 | -    | -     | -     |
| 4                     | 2.92                  | 8.53  | 12.52 | 8.88 | 61.47 | -    | 3.08  | 2.62  |
| 5                     | 3.06                  | 8.33  | 12.68 | 8.60 | 60.23 | -    | 2.92  | 4.18  |
| 6                     | 2.02                  | 6.96  | 15.86 | 9.77 | 55.23 | 0.93 | 5.09  | 4.14  |
| 7                     | 1.33                  | 5.38  | 26.93 | 6.24 | 30.36 | -    | 21.00 | 8.76  |
| 8                     | 3.27                  | 9.19  | 11.00 | 8.49 | 62.40 | -    | 2.43  | 3.22  |
| 9                     | 3.06                  | 5.82  | 15.24 | 9.88 | 59.25 | -    | 3.37  | 3.38  |

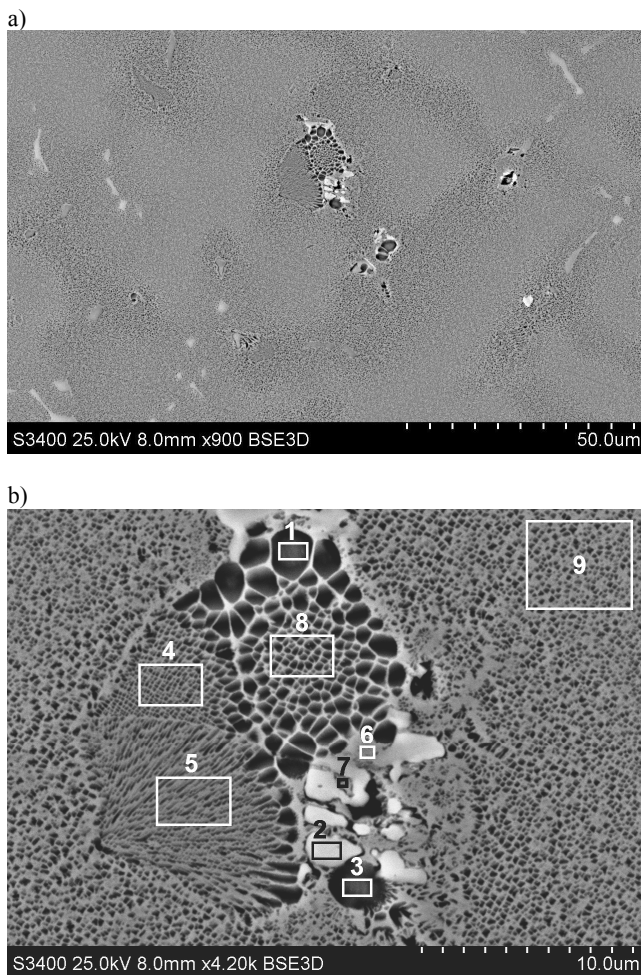


Fig. 4. Microstructure of René 80 superalloy in the as-cast state with areas chosen for EDS analysis (Tab. 3): dendrites of  $\gamma$  phase (a) with  $\gamma$ - $\gamma'$  eutectic and primary MC-type carbides in interdendritic regions (b)

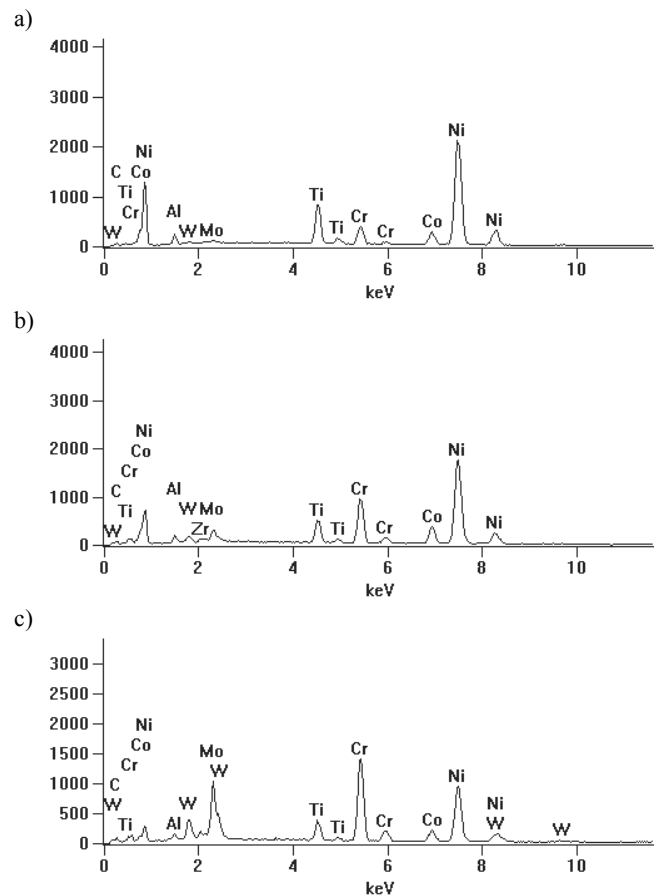


Fig. 5. EDS X-ray spectra in chosen areas: a) area 1; b) area 6; c) area 7 (Fig. 4b, Tab. 3)

Both after the homogenizing-solution heat treatment and after the primary ageing the cuboidal precipitates of primary  $\gamma'$  phase were observed. After the primary ageing there were also observed cuboidal primary  $\gamma'$  precipitates as well as spherical primary  $\gamma'$

precipitates. However hyperfine secondary particles of  $\gamma'$  phase were not visible (probably because of limitations of the equipment).

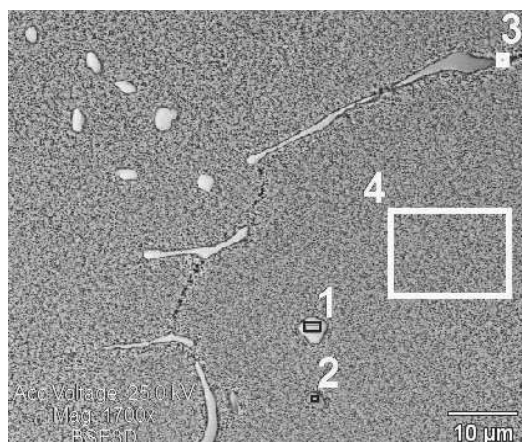


Fig. 6. Microstructure of René 80 superalloy after homogenizing annealing (at 1205°C for 2h) with areas chosen for analysis of the chemical composition (Fig. 7, Tab. 4).

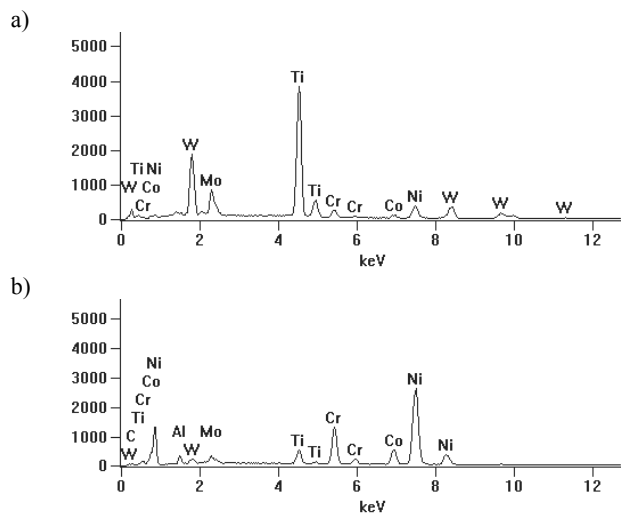


Fig. 7. EDS X-ray spectra in chosen areas a) area 1; b) area 4 (Fig. 6, Tab. 4)

Table 4. Local chemical composition of the alloy after homogenizing annealing - EDS analysis

| Area no. (Fig. 6) | Element content, wt % |       |       |      |       |       |       |
|-------------------|-----------------------|-------|-------|------|-------|-------|-------|
|                   | Al                    | Ti    | Cr    | Co   | Ni    | Mo    | W     |
| 1                 | -                     | 46.34 | 3.59  | 1.30 | 7.00  | 12.34 | 29.42 |
| 2                 | 0.67                  | 40.91 | 6.10  | 2.67 | 17.36 | 14.31 | 17.99 |
| 3                 | 0.64                  | 44.93 | 6.57  | 2.86 | 17.77 | 10.87 | 16.36 |
| 4                 | 2.64                  | 4.67  | 15.04 | 9.81 | 58.60 | 3.28  | 5.97  |

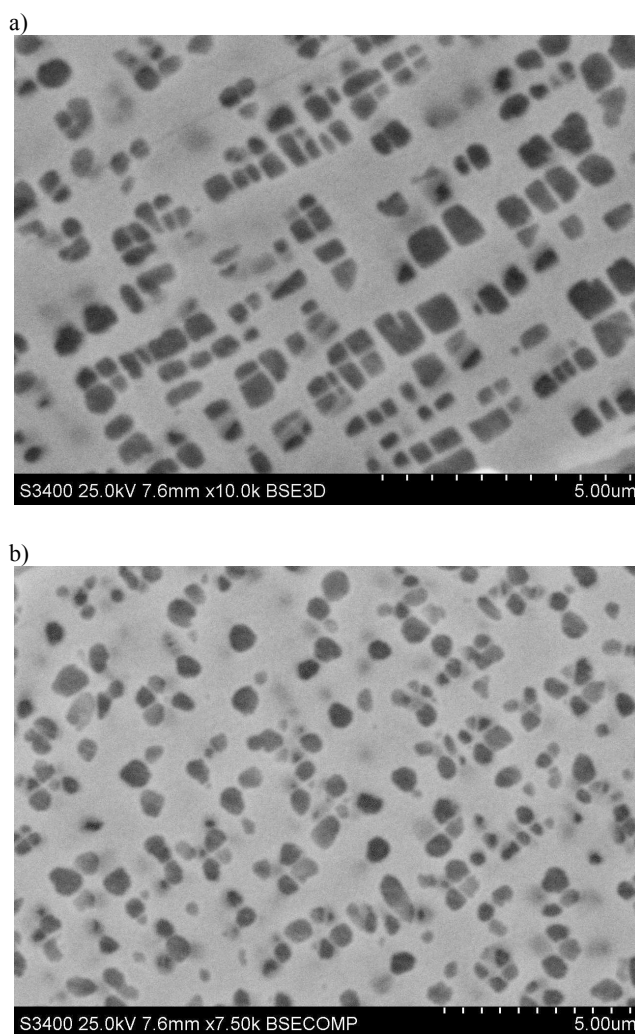


Fig. 8. Various types of morphology of the  $\gamma'$  precipitates after primary aging: a) cuboidal, b) spherical and cuboidal

First trial CVD processes were carried out on the as-cast samples (processes no. 1 and 2 - Tab. 2) varying the temperature. It was found that lower temperature was disadvantageous to the process of the aluminide layer deposition. It caused deterioration of the quality of the outer  $\beta$ -NiAl layer, and resulted in significant increase of its porosity and roughness. Therefore further trials of the coating deposition at a temperature of 950°C were abandoned.

Comparing samples aluminized according to the scheme no. 3 and 4 it was found that after the process no. 3 surface layer was more porous, and a large crack was detected between the additive  $\beta$ -NiAl layer and the diffusion zone (Figs. 11, 12).

The  $\beta$ -NiAl surface layer on the sample no. 4 demonstrated the better quality as well as it was smooth and less porous than the sample no. 3.

For the process no. 5 temperature 1000°C was applied, the same, like for processes no. 3 and 4, however parameters of the flow of gasses were changed - the HCl flow rate was increased from 0.15 nlp/m to 0.6 nlp/m and hydrogen flow rate was reduced from 20-30 nlp/m to 10 nlp/m. Higher pressure was also applied in

the process no.5 (300 mbar). For the process no. 5 as-cast samples were used, as well as samples after homogenizing-solution annealing.

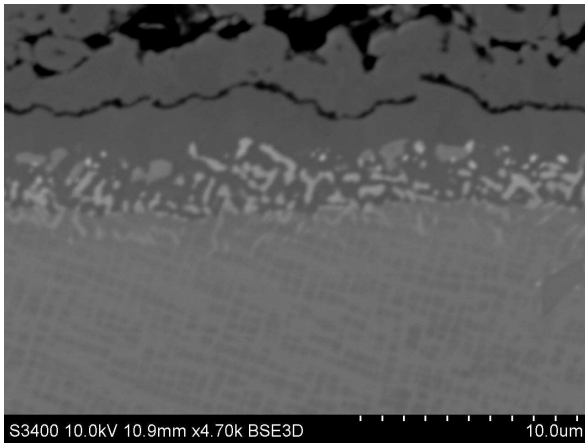


Fig. 9. Microstructure of coated specimen no. 1

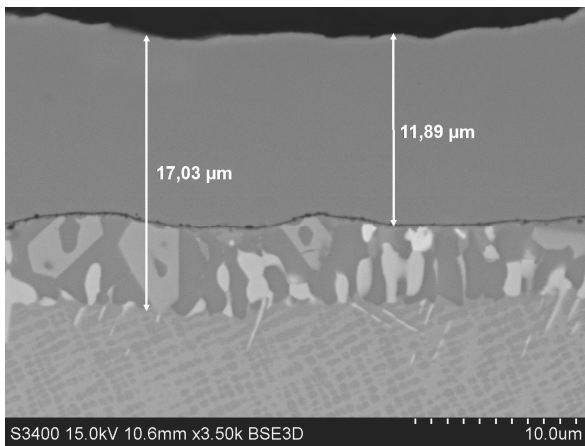


Fig. 10. Microstructure of coated specimen no. 2

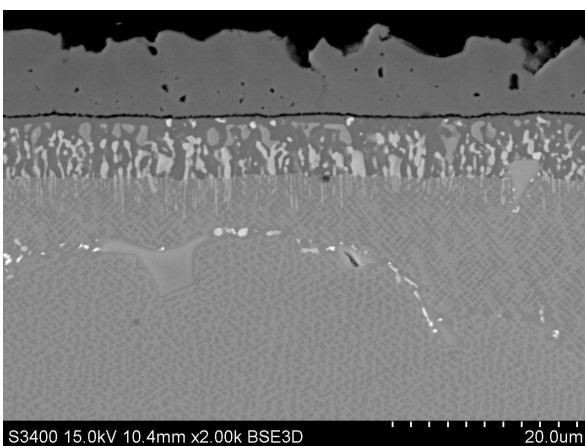


Fig. 11. Microstructure of coated specimen no.3

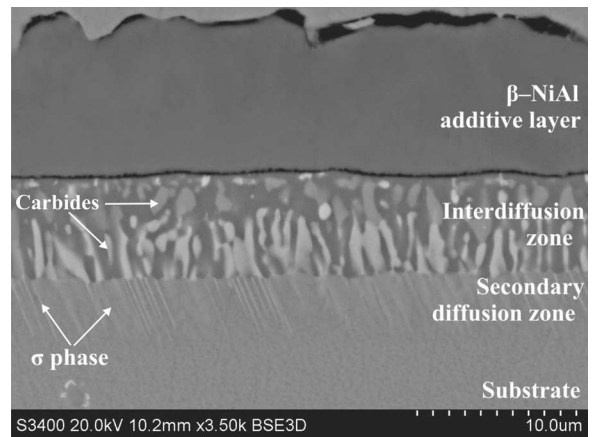


Fig. 12. Microstructure of specimen after homogenizing annealing coated in process no.4

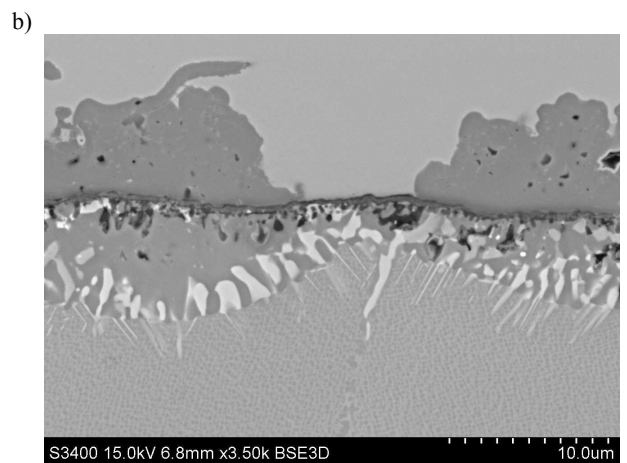
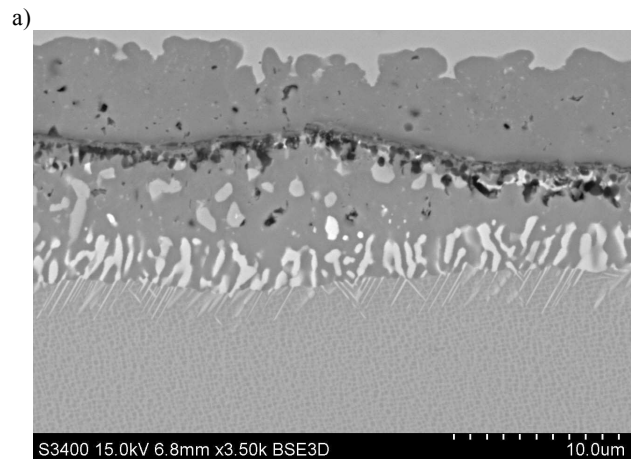


Fig. 13. Microstructure of coated specimen no. 5 - very high porosity of outer layer and diffusion zone (a) and damaged - cracked and spallated surface - discontinuous outer layer (b), both samples were after homogenizing-solutionizing and primary aging heat treatment

It was found that layers on both types of samples, after process no. 3 and no. 5 were very much of inferior quality, i.e. the surface of additive layer was uneven, porosity of the additive layer was high and thickness not uniform (Fig. 13).

After the completed process no. 6 additional diffusion annealing of surface layer was applied at the temperature of 1000°C for 2 h in Ar atmosphere. It was found that in spite of the extra time of annealing, and the interdiffusion of Ni, Al and remaining elements, average thickness of additive layer  $\beta$ -NiAl was still on the satisfactory level, i.e.  $>10\ \mu\text{m}$ . Apart from that, a lower frequency of  $\sigma$  phase precipitates occurrence was noted (Fig. 14).

It is necessary also to recall that the smallest crack between additive-outer layer and diffusion zone was visible in microstructure of sample no. 2 (Fig. 10).

Based on the results of EDS analysis it was found that the content of aluminium in outside layer after the low-activity CVD process amounted to from about 23% up to the 30% by weight. The highest content of Al was after process no. 4, both in the outside additive layer (30.16 wt.%) and in the diffusion zone (25.32 wt.%), and the lowest after the processes no. 1 and no. 5 (Tab. 5). The thickest layer was obtained in the process no. 2 - outer additive layer about  $12\ \mu\text{m}$  thick and total thickness with the diffusion zone about  $17\ \mu\text{m}$ . In the future further processes of aluminizing are planned with application of CVD method (varying the process time and temperature, the flow rate of gasses etc.). The aim will be verification of the kinetics of the growth of aluminide layers and improvement of the quality and properties of the surface layer.

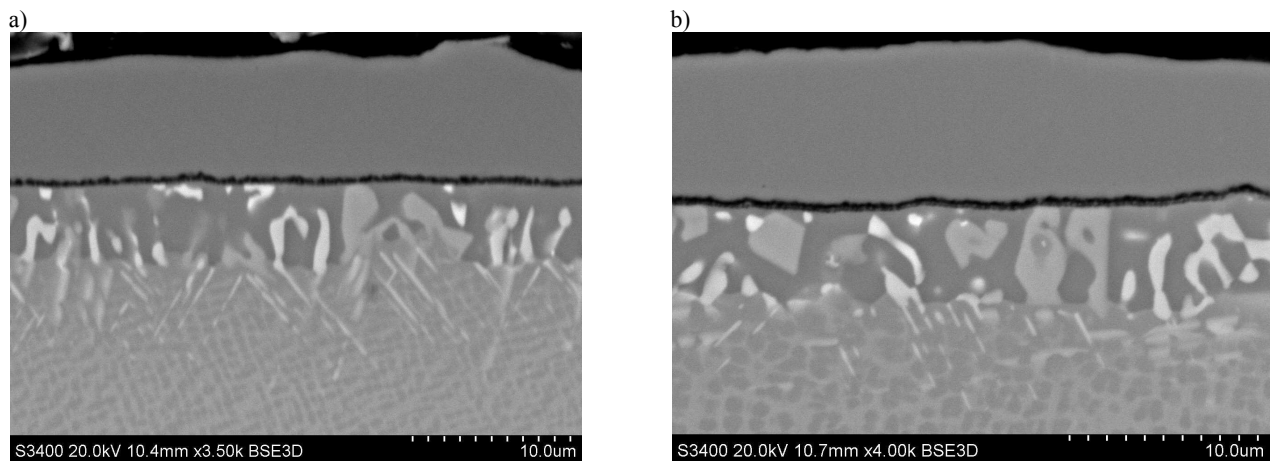


Fig. 14. Microstructures of samples coated in process no. 6, a) in as-cast state, b) after primary aging (both additionally diffusion annealed at 1000°C for 2 h in Ar after CVD process)

Table 5.  
Chemical composition of coated specimens (on cross-sections)

| Proces no. | Location             | wt %  |       |       |      |       |      |      |
|------------|----------------------|-------|-------|-------|------|-------|------|------|
|            |                      | Ni    | Al    | Cr    | Co   | W     | Ti   | Mo   |
| 1          | outer-additive layer | 69.87 | 23.41 | 0.77  | 5.94 |       |      |      |
|            | diffusion zone       | 63.42 | 3.06  | 14.12 | 7.12 | 4.50  | 4.43 | 3.35 |
|            | substrate            | 64.82 | 2.30  | 12.17 | 7.73 | 4.36  | 5.40 | 3.22 |
| 2          | outer-additive layer | 64.30 | 26.07 | 2.34  | 7.30 |       |      |      |
|            | diffusion zone       | 38.36 | 12.12 | 21.25 | 8.06 | 11.62 | 5.38 | 3.21 |
|            | substrate            | 59.36 | 3.07  | 14.93 | 9.06 | 7.07  | 4.80 | 1.15 |
| 3          | outer-additive layer | 64.77 | 27.95 | 1.81  | 5.46 |       |      |      |
|            | diffusion zone       | 44.55 | 13.25 | 16.17 | 8.47 | 6.65  | 6.43 | 4.48 |
|            | substrate            | 59.06 | 2.75  | 14.04 | 9.58 | 5.96  | 4.92 | 3.70 |
| 4          | outer-additive layer | 63.41 | 30.16 | 1.06  | 5.37 |       |      |      |
|            | diffusion zone       | 61.85 | 25.32 | 3.15  | 7.48 |       | 2.21 |      |
|            | substrate            | 48.29 | 7.56  | 15.90 | 9.36 | 7.77  | 5.65 | 5.24 |
| 5          | outer-additive layer | 63.40 | 22.93 | 1.46  | 9.58 |       | 2.63 |      |
|            | diffusion zone       | 46.44 | 8.77  | 17.57 | 8.91 | 9.91  | 4.82 |      |
|            | substrate            | 66.58 | 2.60  | 12.94 | 7.08 | 5.99  | 4.81 | 3.47 |
| 6          | outer-additive layer | 64.04 | 25.16 | 3.13  | 6.99 |       | 0.68 |      |
|            | diffusion zone       | 41.78 | 11.59 | 13.41 | 9.21 | 11.36 | 7.57 | 5.08 |
|            | substrate            | 59.84 | 3.27  | 15.24 | 9.62 | 1.83  | 5.14 | 5.05 |



## 4. Conclusions

On the basis of the results of the studies following conclusions were formulated:

1. Homogenizing annealing at 1205°C for 2 h resulted in more uniform distribution of alloying elements in  $\gamma$  phase and homogeneous microstructure as well as caused dissolving of  $\gamma$ - $\gamma'$  eutectic.
2. The LA CVD processes yield the best results for homogenized alloy.
3. The higher temperature of the LA CVD processes is probably increasing the activity of  $\text{AlCl}_3$  and kinetics of the aluminide layer growth, causing thickening of aluminide layer and outside additive  $\beta$ -NiAl layer.
4. It is possible to regulate the increase in the  $\beta$ -NiAl layer thickness by increasing the HCl amount which is transported to the external generator containing Al granules.
5. In the low-active CVD process it is possible to achieve the most beneficial ratio of the outer layer thickness to the thickness of the diffusion zone applying greater HCl flows and the higher temperature of the process, and presumably also by extending the time.
6. Process of diffusion annealing after the process no. 6, did not cause deterioration of the surface layer quality, additionally to some extent contributed to partial dissolving of the  $\sigma$  phase precipitates.
7. The temperature (1050°C) and the time (4 h) of aluminizing were selected according to the scheme of the heat treatment of René 80 superalloy (temperature 1052°C and time 4h are usually applied in next stage aging treatment - the last stage of heat treatment is secondary aging at temperature 843°C for 16 h).

## Acknowledgements

Financial support of Structural Funds in the Operational Programme - Innovative Economy (IE OP) financed from the European Regional Development Fund - Project "Modern material technologies in aerospace industry", Nr POIG.01.01.02-00-015/08-00 is gratefully acknowledged.

## References

- [1] ASM Specialty Handbook: Nickel, Cobalt, and Their Alloys, ASM International, 2000, 70-81.
- [2] Kh. Rahmani, S. Nategh, Influence of aluminide diffusion coating on low cycle fatigue properties of René 80, *Materials Science and Engineering A* 486 (2008) 686-695.
- [3] Kh. Rahmani, S. Nategh, Isothermal LCF behavior in aluminide diffusion coated René 80 near the DBTT, *Materials and Design* 30 (2009) 1183-1192.
- [4] C.T. Sims, N.S. Stoloff, W.C. Hagel, *Superalloys II*, John Wiley & Sons, Inc., 1987.
- [5] J. Doychak, M. Ruhle, TEM studies of oxidized NiAl and Ni<sub>3</sub>Al cross sections, *Oxidation of Metals* 31 (1989) 431-452.
- [6] G. Sauthoff, *Intermetallics*, Weinheim-New York-Basel - Cambridge-Tokyo, VCH, 1995, 51-67.
- [7] H.J. Grabke, M. Schütze, *Oxidation of Intermetallics*, Wiley-VCH, Weinheim-Berlin-New York, 1997, 79-170.
- [8] G.W. Goward, D.H. Boone, C.S. Giggins, *Trans. ASM* 60 (1967) 228-241.
- [9] G.W. Goward, D.H. Boone, Mechanism of formation of diffusion aluminide coatings on nickel-base superalloys, *Oxidation of Metals* 3 (1971) 475-95.
- [10] J. Sieniawski, Criteria and methods of assessment materials for aviation turbine engine components, Publishing House of Technical University of Rzeszow, Rzeszów, 1995 (in Polish).
- [11] Y. Tamarin, *Protective coatings for turbine blades*, ASM International, 2002.
- [12] J. Sieniawski, Nickel and titanium alloys in aircraft turbine engines, *Advances in Manufacturing Science and Technology* 27/3 (2003) 23-24.
- [13] R. Sivakumar, L.L. Seigle, On the kinetics of the pack-aluminization process. *Metallurgical Transactions A* 7/8 (1976) 1073-1079.
- [14] K.L. Choy, Chemical vapour deposition of coatings, *Progress in Materials Science* 48 (2003) 57-170.
- [15] J-H. Park, T. S. Sudarshan, *Chemical Vapor Deposition*, Surface Engineering Series 2, ASM International, 2001, 1-44.
- [16] W.-P. Sun, H.J. Lin, M.-H. Hon, CVD aluminide nickel, *Metallurgical Transactions A* 17 (1986) 215-220.
- [17] S. Shankar, L.L. Siegle, Interdiffusion and intrinsic diffusion in the NiAl ( $\delta$ ) phase of the Al-Ni system, *Metallurgical Transactions A* 9 (1978) 1467-1476.
- [18] Y. Zhang, J.A. Haynes, B.A. Pint, I.G. Wright, W.Y. Lee, Martensitic transformation in CVD NiAl and (Ni,Pt)Al bond coatings, *Surface and Coatings Technology* 163-164 (2003) 19-24.
- [19] M. Yavorska, J. Sieniawski, Functional properties aluminide layer deposited by CVD method on Inconel 713 LC Ni-base superalloy, *Archives of Materials Science and Engineering* 56 (2011) 187-192.
- [20] M. Zielińska, J. Sieniawski, M. Yavorska, M. Motyka, Influence of chemical composition of nickel based superalloy on the formation of aluminide coatings, *Archives of Materials Science and Engineering* 56/2 (2011) 193-197.
- [21] M. Yavorska, J. Sieniawski, Effect of diffusion on platinum coatings deposited on the surface of nickel based superalloy by the electroplating process, *Archives of Materials Science and Engineering* 44/2 (2010) 5-9.
- [22] M. Zagula-Yavorska, J. Sieniawski, Effect of palladium diffusion in coatings deposited on the nickel based superalloy, *Archives of Materials Science and Engineering* 52/2 (2011) 69-73.
- [23] M. Yavorska, J. Sieniawski, Oxidation behaviour of platinum modified aluminide coatings deposited by CVD method on nickel-based superalloys under air atmosphere, *Journal of Achievements in Materials and Manufacturing Engineering* 46/2 (2011) 204-210.
- [24] G. Moskal, Thermal barrier coatings: characteristics of microstructure and properties, generation and directions of development of bond, *Journal of Achievements in Materials and Manufacturing Engineering* 37/2 (2009) 323-331.
- [25] M. Hetmańczyk, L. Swadźba, B. Mendała, Advanced materials and protective coatings in aero-engines application, *Journal of Achievements in Materials and Manufacturing Engineering* 24/1 (2007) 372-381.
- [26] K. Shirvani, S. Firouzi, A. Rashidghamat, Microstructures and cyclic oxidation behaviour of Pt-free and low-Pt NiAl coatings on the Ni-base superalloy Rene-80, *Corrosion Science* 55 (2012) 378-384.